Role of the [65−72] Disulfide Bond in Oxidative Folding of Bovine Pancreatic Ribonuclease A†

Hang-Cheol Shin,‡ Mahesh Narayan, Myeong-Cheol Song, and Harold A. Scheraga*

Baker Laboratory of Chemistry and Chemical Biology, Cornell University, Ithaca, New York 14853-1301

Received June 18, 2003

ABSTRACT: To assess the role of the [65−72] disulfide bond in the oxidative folding of RNase A, use has been made of [C65S, C72S], a three-disulfide-containing mutant of RNase A which regenerates from its two-disulfide precursor in an oxidation and conformational folding-coupled rate-determining step. The distribution of disulfide bonds in the one-disulfide-containing ensemble of this mutant has been characterized. In general, the disulfide-bond distribution in its 1S ensemble agrees relatively well with the corresponding distribution in wt-RNase A and with distributions based on calculations of loop entropy, except for the absence of the [65−72] disulfide bond. There is no bias (over the entropic influence) for the three native disulfide bonds, [26−84], [40−95], and [58−110]. Previous oxidative folding results for wt-RNase A indicated the predominance of the des [40−95] intermediate over des [65−72] after the rate-determining step in the regeneration process. Considering that there is no preferential distribution of disulfides in the 1S ensemble of [C65S, C72S], in contrast to the preferential population of the [65−72] disulfide bond in wt-RNase A, these results indicate a critical role for the [65−72] disulfide bond in the regeneration of wt-RNase A. Furthermore, analysis of the disulfide distribution of the 1S intermediates of [C65S, C72S] compared to that of wt-RNase A lends support for a physicochemical basis for the previously observed slow folding rate of this mutant, compared to its analogue (des [65−72]) of wt-RNase A.

Bovine pancreatic ribonuclease A (RNase A)[1] is a small protein that contains four disulfide bonds at positions [26−84], [40−95], [58−110], and [65−72]. Among the various observed pathways for the oxidative folding of RNase A, the dominant one (to the extent of about 80%) involves the early formation of the [65−72] disulfide bond to a considerable extent in the 1S ensemble, and the subsequent formation of des [40−95] (a three-disulfide nativelike intermediate) by thiol-disulfide reshuffling reactions of the 3S ensemble in the rate-determining step (*1*, *2*). A minor, albeit parallel pathway (to the extent of about 20%) involves the formation of des [65−72] (another three-disulfide nativelike intermediate) in the rate-determining step by similar thiol-disulfide reshuffling reactions of the 3S ensemble (*1*, *2*). Both des [40−95] and des [65−72] are then oxidized to the native protein (*1*, *2*).

Two very minor pathways (to the extent of at most 5% each) involve the formation of des [40−95] and des [65−72], respectively, by direct oxidation of the 2S ensemble (*3*, *4*). These very minor pathways are too small to detect in folding experiments with wild-type RNase A but could be observed directly only in oxidative folding studies (*3*, *4*) of the mutants [C65S, C72S], [C65A, C72A] and [C40A, C95A]. The importance of the [65−72] disulfide bond in the early stages of folding of wild-type RNase A is demonstrated by, among other things, the very slow rate of folding of the [C65S, C72S] and [C65A, C72A] mutants compared to that of the wild-type protein (*3*, *4*).

While the oxidative folding pathways of several proteins have been studied by following the kinetics of the regeneration process (*5*−*9*), analysis of the disulfide-bond distributions of unstructured intermediates [in addition to other techniques (*10*−*13*)] in the regeneration process provided valuable information about the enthalpic interactions in unstructured intermediates (*14*−*19*). In RNase A, with the exception of des [40−95] and des [65−72], all other intermediates (i.e., 1S, 2S, and 3S) and R, which accumulate during regeneration at 25 °C, are unstructured (*20*−*24*). Disulfide mapping studies of the 1S and 2S ensembles of wild-type RNase A (*14*, *16*) and of its three-disulfide mutant [C40A, C95A] (*19*) reveal that the [65−72] bond is the predominant disulfide bond in unstructured intermediates [for example, it is present to the extent of 40% of the 1S ensemble

† This work was supported by the National Institute of General Medical Sciences of the National Institutes of Health (Grant No. GM-24893). Support was also received from the National Foundation for Cancer Research.

* To whom correspondence should be addressed: Tel. (607) 255-4034; Fax (607) 254-4700; E-mail: has5@cornell.edu.

‡ Present Address: Department of Bioinformatics and Life Science, Soongsil University, Seoul 156-743, Korea.

[1] Abbreviations: RNase A, bovine pancreatic ribonuclease A; wt, wild-type; des [x−y], wild-type RNase A in which the disulfide bond indicated as [x−y] is reduced; nS, the ensemble of disulfide species with n disulfide bonds; [C40A, C95A], the three-disulfide mutant of RNase A in which cysteines 40 and 95 have been replaced by alanines; [C65S, C72S], the three-disulfide mutant of RNase A in which cysteines 65 and 72 have been replaced by serines; [C65A, C72A], the three-disulfide mutant of RNase A in which cysteines 65 and 72 have been replaced by alanines; des species, a species having all but one of the native disulfides in RNase A; 3S*, symbol for a des species; DTT^{red}, reduced dithiothreitol; DTT^{ox}, oxidized dithiothreitol; GdnSCN, guanidine thiocyanate; AEMTS, 2-aminoethyl methanethiosulfonate; DDS, disulfide-detection system; MS, mass spectrometry; MALDI-TOF, matrix-assisted laser desorption ionization-time-of-flight; NTSB, disodium 2-nitro-5-thiosulfobenzoate.

10.1021/bi030152h CCC: $25.00
Published on Web 09/10/2003

of wild-type RNase A (*14*)].

It is, therefore, of interest to determine the distribution of one-disulfide bonds in the 1S ensemble of a mutant, such as [C65S, C72S], that does not contain the [65−72] disulfide bond, and to assess the basis for the low rate of oxidative folding of this mutant as compared to both wild-type RNase A and [C40A, C95A] (*2*−*4*). Besides the importance of this question for the folding of wild-type RNase A, it is also relevant to the oxidative folding of the homologues, onconase and angiogenin, neither of which contains the [65−72] disulfide bond.

Here we report the relative populations of the 1S disulfide-bond distributions of the [C65S, C72S] mutant of RNase A, an analogue of des [65−72]. The resulting data and their implications for the refolding process of RNase A and for multi-disulfide-containing proteins are discussed.

EXPERIMENTAL PROCEDURES

Materials. The [C65S, C72S] mutant was expressed and purified by the procedures described by Laity et al. (*25*). The purity of the mutant protein was confirmed by cation-exchange HPLC. Ultrapure DTT^{red} was obtained from Sigma, and DTT^{ox} (Sigma) was purified by the method of Creighton (*26*). AEMTS was synthesized as described by Bruice and Kenyon (*27*). Trypsin (type IX, from porcine pancreas) and α-chymotrypsin (type II, from bovine pancreas) from Sigma were used without further purification. All other reagents were of the highest grade commercially available and were used without further purification.

Reduction of [C65S, C72S] Mutant. Fully reduced [C65S, C72S] was obtained by adding 30 mg of the mutant protein to 2 mL of 100 mM DTT^{red} solution in a buffer containing 100 mM Tris-acetate, 2 mM EDTA, and 4 M GdnSCN at pH 8.0 and 25 °C and maintained in this buffer for 3 h. The mixture was then desalted using 100 mM acetic acid on a Sephadex G-25 Superfine column with continuous sparging of argon. The reduced protein was immediately frozen and lyophilized. The resulting protein was reconstituted into 100 mM acetic acid at a concentration of 5 mg/mL and stored at −70 °C. The purity of the reduced protein was checked by blocking an aliquot of the reduced protein with a 50−100-fold molar excess of AEMTS at pH 8.0, followed by ion-exchange HPLC analysis. No oxidized protein was detected.

Isolation of One-Disulfide Intermediates and Proteolytic Digestion. The protein was refolded at a concentration of 25 μM in a solution of 100 mM DTT^{ox}, 100 mM Tris-acetate, and 2 mM EDTA at pH 8.0. The oxidation reaction was quenched at 60 min with a 100-fold molar excess of AEMTS over protein. These conditions were chosen to produce a maximum yield of 1S intermediates. Because of the positive charge added to each of the free protein thiols after blocking with AEMTS, the disulfide groupings are well separated using cation-exchange HPLC. Both blocked one-disulfide intermediates and the fully reduced and blocked [C65S, C72S] mutant were lyophilized and reconstituted into 100 mM Tris-acetate buffer at pH 8.0 prior to digestion. The typical protein concentration was approximately 0.5 mg/mL. Digestion was first carried out with trypsin (at an enzyme/substrate mass ratio of 1/50) for 2 h and then with α-chymotrypsin at the same concentration for another 2 h. The pH of the solution was then lowered to 2 with 20% (v/v) TFA. The digested mixture was stored at −70 °C.

Peptide Mapping. The digests were analyzed using reverse-phase HPLC (with a Hewlett-Packard series 1100 system, with a binary pump and a diode array detector). Absorbance was monitored at 215 nm. A YMC mini-bore column (ODS AQ 120A S3, 2 mm × 150 mm) was used with a binary gradient. First, 100% buffer A (99.95% H_2O, 0.05% TFA) and 0% buffer B (50% acetonitrile, 0.05% TFA) were run isocratically (0.2 mL/min) for 10 min, followed by a change to 90% B over 300 min. All peaks from both the reduced-blocked (standard) and one-disulfide digestion chromatograms were collected and lyophilized separately and subjected to MALDI-TOF mass analysis using a Bruker BIOFLEX III mass spectrometer. The masses determined with the instrument have an error of less than ± 0.1%.

Disulfide Bond Analysis. The amounts of material in the disulfide-containing fragments from the HPLC chromatograms of both the reduced-blocked (standard) and one-disulfide protein digestion were determined quantitatively. A disulfide detection system (DDS) was connected in series with the UV detector. The details of the DDS were described by Thannhauser et al. (*28*). This system consisted of a solution (0.5 M Na_2SO_3, 2 mM EDTA, 0.5 mM NTSB, 200 mM glycine, pH 9.5) pumped isocratically (HP 1100, quaternary pump, 0.5 mL/min) to a tee-fitting, which mixed this solution with effluent from the detector of the reverse-phase HPLC system. The mixed solution then proceeded through a 30 s reaction loop (0.01 in. i.d.) to the detector (HP 1100 variable wavelength, 410 nm). The signal from the DDS detector is proportional to the number of moles of disulfide bonds eluting at a given time. Therefore, the concentrations of peptides can then be determined quantitatively on the basis of the number of disulfide bonds that they contain.

RESULTS

Refolding Experiments. The kinetics of oxidative refolding of RNase A and its des mutant analogues have been studied in great detail (*1*−*4*, *29*−*32*). Using the kinetic parameters and DTT^{ox} concentration dependence of the refolding rate of [C65S, C72S], we were able to select conditions under which the formation of 1S (ensemble of one-disulfide intermediates) is maximized. A typical ion-exchange chromatogram is shown in Figure 1. The peak identities have been assigned previously (*3*) and are labeled on the Figure. The typical yield of the 1S ensemble is about 50% (of the total protein).

Peptide Mapping. The digestion map monitored by UV absorption and the corresponding DDS chromatogram (used as a measure of the concentrations of disulfide-containing peptides) of the digested 1S intermediates are displayed in panels a and b of Figure 2, respectively. Each peak in the DDS map containing disulfide-bonded peptides is labeled, and Table 1 lists the corresponding peak compositions, along with their observed and calculated masses. All theoretically possible disulfide bonds are present in the isolated 1S ensemble. The identity of each peak was determined by matching a table of theoretically possible masses to the observed mass, and the identities were confirmed by reduction and reblocking experiments as described previously (*14*, *16*). The reduction and reblocking process is a necessary step to determine the quantitative composition of each peak in

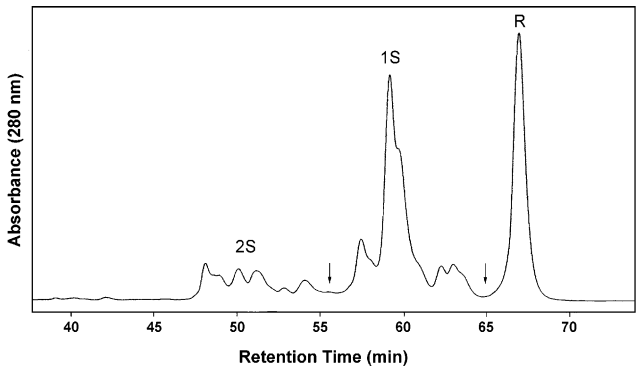

FIGURE 1: Cation-exchange chromatogram for refolding of the [C65S, C72S] mutant (with 100 mM DTT^{ox} and 25 μM reduced [C65S, C72S] at pH 8.0 and 25 °C) quenched and blocked at 60 min. R, 1S and 2S represent the AEMTS-blocked reduced, one- and two-disulfide intermediates, respectively. The arrows indicate the portion that was isolated as the 1S ensemble. The refolding mixture was quenched before the appearance of more oxidized species.

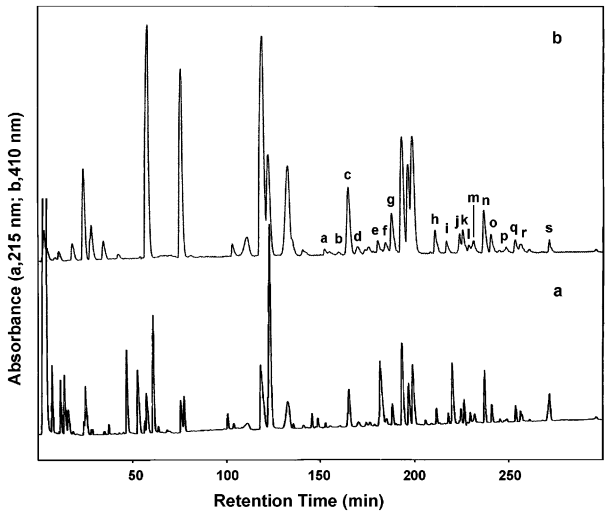

FIGURE 2: A typical reversed-phase HPLC chromatogram of the one-disulfide intermediates after tryptic/chymotryptic digestion. The bottom chromatogram (a) shows the UV absorbance at 215 nm, and the top (b) shows the corresponding DDS signal. Letters denote peaks that contain intrapeptide disulfide bonds, and correspond to the letters used in Table 1. Unlabeled peaks contain either only AEMTS-blocked protein or no disulfide bonds at all.

the map, because some peaks contain several fragments. The unlabeled peaks contain either AEMTS-blocked protein only or no disulfide bonds at all.

Distribution of One-Disulfide Intermediates. To assess the contribution of specific conformational effects to the stability of the various one-disulfide species, it is useful to compare the experimentally observed distribution of one-disulfide species to the expected random distribution. The random distribution depends on the size of the loops created by formation of the disulfide bonds and can be determined by calculating the loop entropy involved in the formation of all possible one-disulfide species (*14*, *33*). The relative populations of the one-disulfide bonds in the 1S ensemble are summarized in Table 2. The experimentally determined disulfide-bond populations in the 1S ensemble of wild-type RNase A (*14*) are normalized and also shown for comparison (Table 2). The normalization was carried out so that the sum of the percentages in the ensemble of wild-type 1S is equal to 100, i.e. disulfide bonds involving Cys65 or Cys72 in the wild-type 1S ensemble are not counted.

DISCUSSION

The Unstructured Ensembles of RNase A. This study is a continuation of our investigations into the conformational propensities of reduced RNase A and its unstructured intermediates under folding conditions. Here, we have mapped the 1S distribution of a slow-folding three-disulfide-containing mutant of RNase A that lacks the disulfide bond [65−72], and the results suggest an important implication for the role of this bond in the regeneration of reduced RNase A.

In the 1S and 2S ensembles of wt-RNase A, the disulfide bond [65−72] is favored over all other disulfide bonds by both entropic and enthalpic contributions (*14*, *16*). The short distance between residues 65 and 72 involves the least loss of entropy after formation of this disulfide as compared to other disulfides (except [58−65] which has the same number of residues in the loop). In previous studies involving a short peptide (residues 58−72) containing cysteines 58, 65, and 72, the propensities to form bonds [65−72] and [58−65] were the same as in the entire RNase A chain (residues 1−124), indicating that the enthalpic interactions promoting the formation of the [65−72] disulfide bond were present within this sequence and any long-range interactions were insignificant (*34*). NMR studies of the short segment that contained cysteines 65 and 72 indicated the presence of a type II β-turn formed from residues 66−69 (*35*). Interestingly, in native RNase A, a type III β-turn is formed from residues 65−68 (*36*). Recent modeling work has revealed the presence of critical hydrogen-bonding interactions within residues in the loop that act as strong conformational determinants that dictate the formation of the disulfide bond [65−72] (*37*). This result is verified by experimental disulfide bond distributions of the 1S, 2S, and 3S ensembles of [C40A, C95A] where the [65−72] bond was found to be much more strongly favored than that predicted by the power-law dependence on loop length (*19*).

Role of Bond [65−72] in the Oxidative Folding of RNase A. The predominant role of the disulfide bond [65−72] can easily be evaluated (a) from kinetic data gathered from the oxidative folding of wild-type RNase A and (b) by comparison of the regeneration rates of its three-disulfide-containing mutant analogues, [C40A, C95A], [C65A, C72A], and [C65S, C72S] (*2*−*4*).

(a) Wild-type regeneration studies at 25 °C revealed the presence of two structured des intermediates emerging from reshuffling reactions that qualify as the rate-determining steps in the oxidative folding of RNase A (*1*, *2*). Of these two des species, des [40−95] which lacks the [40−95] disulfide bond (but retains the [65−72] bond) constituted about 80% of the total, and regenerated with an observed forward rate constant of $k_f^{obs} = 1.4 \pm 0.1 \times 10^{-2}$ min^{-1} from its 3S isomers (*2*); the des [65−72] intermediate (lacking the bond [65−72]) constituted about 20% of the total, and regenerated from its 3S isomers with a $k_f^{obs} = 0.21 \pm 0.02 \times 10^{-2}$ min^{-1} (*2*).

(b) Furthermore, [C65S, C72S] and [C65A, C72A] (both lacking [65−72]) regenerate from their 2S isomers with rate-constants that are 4- to 5-fold lower than the rate constant for the regeneration of [C40A, C95A] (possessing [65−72]) (*3*, *4*).

Table 1: Tryptic−Chymotryptic Digestion Fragments of One-Disulfide Intermediates

peak[a]	mass	assignment	expected mass	disulfide	fraction	peak[a]	mass	assignment	expected mass	disulfide	fraction
a	1447	(26−31, 80−85)	1448	[26, 84]	0.018	j	2305	(47−61, 80−85)	2307	[58, 84]	0.037
b	2198	(26−31, 86−98)	2200	[26, 95]	0.012	k	1907	(80−85, 105−115)	1908	[84, 110]	0.060
c	1549	(80−85, 92−98)	1552	[84, 95]	0.220	l	2659	(86−98, 105−115)	2662	[95, 110]	0.017
d	2139	(80−85, 86−98)	2141	[84, 95]	0.031	m	2470	(47−61, 92−98)	2470	[58, 95]	0.039
e	1500	(40−46, 80−85)	1499	[40, 84]	0.039	n	2070	(92−98, 105−115)	2071	[95, 110]	0.110
f	1421	(80−85, 92−97)	1423	[84, 95]	0.040	o	2419	(40−46, 47−61)	2420	[40, 58]	0.047
g	1559	(26−31, 40−46)	1560	[26, 40]	0.074	p	2696	(38−46, 47−61)	2695	[40, 58]	0.016
	1831	(26−31, 38−46)	1832	[26, 40]	0.018		2624	(47−61, 77−85)	2625	[58, 84]	0.009
	2252	(40−46, 86−98)	2254	[40, 95]	0.031	q	2020	(40−46, 105−115)	2022	[40, 110]	0.033
h	2370	(26−31, 47−61)	2366	[26, 58]	0.060	r	2225	(77−85, 105−115)	2227	[84, 110]	0.033
I	1967	(26−31, 105−115)	1968	[26, 110]	0.028	s	2826	(47−61, 105−115)	2828	[58, 110]	0.028

[a] The peak labels correspond to those in Figure 2b.

Table 2: Distribution of One-Disulfide Intermediates in the Refolding of [C65S, C72S]

disulfide bond[a]	experimental percentage[b]	random percentage[c]	ratio[d]	wt 1S[e] percentage
26−40	9.2	16.3	0.6	12.2
26−58	6.0	4.7	1.3	7.9
26−84	1.8	1.9	0.9	4.0
26−95	1.2	1.4	0.9	3.4
26−110	2.8	1.1	2.5	3.0
40−58	6.3	11.3	0.6	7.9
40−84	3.9	3.3	1.2	ND[f]
40−95	3.1	2.2	1.4	3.7
40−110	3.3	1.4	2.4	5.5
58−84	4.6	6.3	0.7	7.3
58−95	3.9	3.9	1.0	1.8
58−110	2.8	2.2	1.3	4.6
84−95	29.1	23	1.3	26.2
84−110	9.3	6.3	1.5	0.9
95−110	12.7	14.6	0.9	11.6

[a] Boldface type indicates the three native disulfide bonds. [b] The experimentally determined value for the percent of total disulfide bonds having the listed bond. [c] The random percentage represents the random distribution calculated by considering only the loop entropy. [d] Ratio of the experimentally determined percentage to the random percentage. [e] The wt 1S column represents the experimentally determined disulfide-bond populations in the 1S ensemble of wild-type RNase A by Xu et al. (*14*) normalized so that the sum of percentages in this column equals 100%, i.e., disulfide bonds involving Cys65 or Cys72 in the wild-type 1S ensemble are not counted. [f] ND indicates that the populations for these species were not determined, since they could not be detected experimentally by Xu et al. (*14*).

These data are indicative of the critical role of the [65−72] disulfide bond since (1) it is a predominant disulfide bond in the unstructured 1S and 2S ensembles, (2) a structured intermediate lacking that bond (viz., des [65−72]) regenerates ~7-fold slower than a structured intermediate containing the bond (viz., des [40−95]), and (3) three-disulfide mutants lacking [65−72] fold about half an order of magnitude slower than the three-disulfide mutant that retains [65−72]. [It should be noted that thermodynamic stability is not an issue here since the midpoints of their respective thermal transitions (i.e., T_m's for des [40−95] and des [65−72]) are almost equal and well above the temperature at which the experiments were carried out (*25*)].

However, a deeper analysis reveals that it is not possible to pinpoint the smaller rate of formation and lower significance of the des [65−72] pathway (compared to the des [40−95] pathway) as resulting merely from the absence of the [65−72] disulfide bond. This is because, in molecules lacking [65−72], some other nonnative disulfide bond may have acquired predominance and would need to reshuffle to a native disulfide bond to be able to fold. Obviously, we cannot determine the disulfide-bond distributions in those molecules of the wild-type protein that lack only [65−72] to see the effects of its absence on the (re)distribution of other disulfides. Nevertheless, such a scenario cannot account for the slow folding of [C40A, C95A] as compared to its wild-type intermediate analogue des [40−95] because the disulfide-bond distributions for the unstructured one-disulfide ensembles of this mutant were in good-agreement with the corresponding distributions for the wild-type molecule (*19*). The reason for the slow folding of [C40A, C95A] compared to that of the analogue, des [40−95], is also explained later in the Discussion.

In this study, the [65−72] disulfide bond was deleted by replacing cysteine residues at positions 65 and 72 by serine residues. By investigating the 1S disulfide-bond distributions of [C65S, C72S], which simulates the wild-type intermediate des [65−72], we can assess the conformational propensities toward the formation of des [65−72] and the effect of the deletion of the [65−72] disulfide bond on the oxidative refolding of reduced RNase A.

Our results in Table 2 show that all 15 theoretically possible one-disulfide species are formed in the refolding of the [C65S, C72S] mutant in the presence of DTT^{ox}. The relative populations of the disulfide bonds in the 1S ensemble of [C65S, C72S] are compared with those of the corresponding disulfide bonds in the 1S ensemble of wild-type RNase A and those determined by calculating the loop entropy involved in the formation of all possible one-disulfide species. The 1S disulfide-bond populations for the [C65S, C72S] mutant generally agree with those of wild-type RNase A and with a random distribution. However, the populations of some disulfide bonds in the wild-type distribution do not agree with corresponding ones in the mutant distribution; most notably, the [40−84] disulfide bond, which was not detected in the 1S intermediates of the wild-type RNase A, appears as a peptide fragment having the [40−46] and [80−85] fragments joined by a disulfide bond (e in Table 1). Nevertheless, the population of the [40−84] disulfide bond in the 1S ensemble of [C65S, C72S] agrees well with the random value calculated from loop entropy (3.9 vs 3.3%) (see Table 2). Another discrepancy appears in the [84−110] disulfide bond, which is reasonably well populated in the mutant (9.3%), but is much less populated in the wild-type RNase A (1%). In fact, the population of the [84−110] disulfide bond in the 1S ensemble of [C65S, C72S] is in better agreement with that calculated from loop entropy, compared to that in the 1S ensemble of wild-type RNase A.

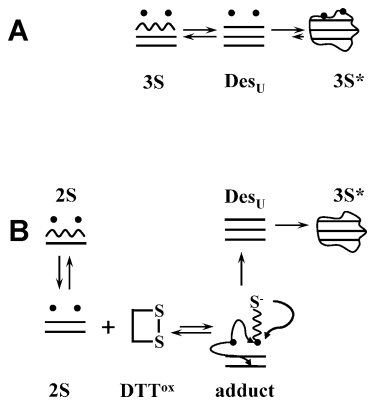

FIGURE 3: (A) Formation of des [65−72], i.e., 3S*, from its 3S isomers. ——, native disulfide bond; wavy line, nonnative disulfide bond; ●, free thiol. (B) Formation of [C65S, C72S] from its 2S precursors. ——, native disulfide bond; wavy line, nonnative disulfide bond; ●, free thiol.

Nevertheless, the predominant nature of this nonnative bond does not appear to be a major reason for the lesser importance of the des [65−72] pathway. This is because its population is still only about 25% of the amount of [65−72] that is normally present in the 1S distribution of wild-type protein (9.3% compared to 40%). In other words, we would need 40% of a nonnative bond to compensate for the loss of the native [65−72] bond for such a nonnative bond to be the sole influence for the percentage of des [65−72] formed or for its rate of formation to be 7-fold slower than that of des [40−95].

Understanding the Nature of Rate-Determining Steps. Overall, the distribution pattern of one-disulfide intermediates in the [C65S, C72S] mutant generally agrees with that calculated from the loop entropy involved in the formation of all possible one-disulfide species. Such an agreement of the overall distributions in the 1S ensemble for wild-type protein and [C65S, C72S] has important implications for the observed slow folding rate of [C65S, C72S] as compared to the folding rate for its analogue, des [65−72]. Des [65−72] is formed from its three-disulfide isomers (3S) by a redox-independent, rate-determining reshuffling reaction (3S→3S*) (*1*, *2*). The observed rate constant for its formation, k_f^{obs} is $0.21 \pm 0.02 \times 10^{-2}$ min^{-1} (*2*). On the other hand [C65S, C72S] regenerates from its 2S precursors by an oxidation and conformational-folding-coupled rate-limiting step (2S→3S*) with an observed rate constant of $0.1 \pm 0.01 \times 10^{-2}$ min^{-1} M^{-1} (*3*). The maximal rate for such a step can be achieved at a saturating concentration of DTT^{ox} (200 mM) to give a forward rate of $0.2 \times 0.1 \times 10^{-2}$ min^{-1}, i.e., 0.02×10^{-2} min^{-1}. This rate is still ∼10-fold slower than that achieved for the wild-type analogue (i.e., 0.21×10^{-2} min^{-1})

While spurious effects of mutating the two cysteines to serines in the mutant analogues might serve as an explanation for the difference in the results, given the general agreement between the disulfide distributions of the 1S ensembles of [C65S, C72S] and wt-type RNase A, such a hypothesis must be ruled out. Instead, we turn our attention to the nature of the respective rate-determining steps for des [65−72] and [C65S, C72S].

In the rate-determining step of des [65−72], there exists a competition between reshuffling reactions and conformational folding (Figure 3 A). At the moment of the formation of the third native bond in this molecule (from its two native and one nonnative disulfide-containing 3S precursor isomer) to produce an unfolded native disulfide-containing species [Des$_U$ (*38*) in Figure 3A], that fraction of Des$_U$ molecules that have all their prolines in the right conformation are able to fold very fast and lock the disulfides in a stable structure, preventing their reshuffling. This is simply because the conformational folding for such species is on the milliseconds time-scale (*39*, *40*) and is therefore able to out-compete the back-reshuffling reaction which takes place on the seconds time-scale (*41*).

The rate-determining step for the three-disulfide mutant [C65S, C72S] is very different from its analogue, des [65−72]. In the rate-determining step for this mutant analogue, there exists a competition between reshuffling reactions and the two-step oxidation reaction (Figure 3B). [C65S, C72S] regenerates by "oxidatively folding" from its 2S precursors (2S→3S*, where 3S* is [C65S, C72S]). It can do so only by oxidation of those 2S molecules that contain only native disulfides. Such native disulfide-containing 2S molecules are in equilibrium with other 2S isomers. To form [C65S, C72S], a molecule of DTT^{ox} must form a mixed disulfide with one of the two remaining free cysteines of a 2S molecule that contains only native disulfides. Such a mixed disulfide with DTT^{ox} is very unstable, given the tendency of the redox reagent to cyclize (thick arrow in Figure 3B). For successful oxidation, the free thiol of the 2S molecule must attack the mixed disulfide to liberate DTT^{red} (thin arrow in Figure 3B). During this two-step process (i.e., formation of an adduct and liberation of DTT^{red}), intramolecular reshuffling between the exposed native disulfides and the remaining free cysteine (reaction indicated by the dashed arrows) in the unstructured 2S molecule is free to take place and effectively competes with the oxidation process. Therefore, the observed rate-constant for such an oxidation and conformational folding-coupled step (Figure 3B) is much slower than for a purely reshuffling and conformational-folding coupled system (Figure 3A).

Such an argument also holds for explaining the slow regeneration rate of the three-disulfide mutant [C40A, C95A] as compared to that of des [40−95].

In conclusion, we have measured the distribution of the one-disulfide intermediates present in the 1S ensemble that is populated during the oxidative refolding of the [C65S, C72S] mutant of RNase A. All 15 theoretically possible one-disulfide couplings are observed, and the disulfide-bond percentages in the 1S ensemble of [C65S, C72S] agree relatively well with those for the corresponding disulfide bonds in the 1S ensemble of wild-type RNase A and those determined by calculating the loop entropy involved in the formation of all possible one-disulfide species. The random distribution of one-disulfide intermediates in [C65S, C72S] with no particular preference for the native disulfide bonds ([26−84], [40−95], [58−110]), along with the significantly slow folding-rate of the wt-intermediate des [65−72], sheds light on the critical role of the [65−72] disulfide bond in the oxidative refolding of wt-RNase A. The mapping results have also clarified the characteristics that are required for successful regeneration of proteins in general by allowing us to distinguish clearly between the intricate mechanisms of different rate-determining steps that are possible in the oxidative folding of multi-disulfide-containing proteins.

ACKNOWLEDGMENT

We thank Dr. Guoqiang Xu for help with Figure 3 A and B.

REFERENCES

1. Rothwarf, D. M., Li, Y.-J., and Scheraga, H. A. (1998) *Biochemistry 37*, 3760−3766.
2. Rothwarf, D. M., Li, Y.-J., and Scheraga, H. A. (1998) *Biochemistry 37*, 3767−3776.
3. Iwaoka, M., Juminaga, D., and Scheraga, H. A. (1998) *Biochemistry 37*, 4490−4501.
4. Xu, X., and Scheraga, H. A. (1998) *Biochemistry 37*, 7561−7571.
5. Pace, C. N., and Creighton, T. E. (1986) *J. Mol. Biol. 188*, 477−486.
6. Pace, C. N., Grimsley, G. R., Thomson, J. A., and Barnett, B. J. (1988) *J. Biol. Chem. 263*, 11820−11825.
7. Oas, T. G., and Kim, P. S. (1988) *Nature 336*, 42−48.
8. Thannhauser, T. W., Rothwarf, D. M., Scheraga, H. A. (1997) *Biochemistry 36*, 2154−2165.
9. Dadlez, M. (1997) *Acta Biochim. Pol. 44*, 433−452.
10. Navon, A., Ittah, V., Landsman, P., Scheraga, H. A., and Haas, E. (2001) *Biochemistry 40*, 105−118.
11. Navon, A., Ittah, V., Scheraga, H. A., and Haas, E. (2002) *Biochemistry 41*, 14225−14231.
12. Narayan, M., Welker, E., and Scheraga, H. A. (2003) *J. Am. Chem. Soc. 125*, 2036−2037.
13. Narayan, M., Welker, E., and Scheraga, H. A. (2003) *Biochemistry 42*, 6947−6955.
14. Xu, X., Rothwarf, D. M., and Scheraga, H. A. (1996) *Biochemistry 35*, 6406−6417.
15. Ruoppolo, M., Torella, C., Kanda, F., Panico, M., Pucci, P., Marino, G., and Morris, H. R. (1996) *Folding Des. 1*, 381−390.
16. Volles, M. J., Xu, X., and Scheraga, H. A. (1999) *Biochemistry 38*, 7284−7293.
17. Ruoppolo, M., Vinci, F., Klink, T. A., Raines, R. T., and Marino, G. (2000) *Biochemistry 39*, 12033−12042.
18. Vinci, F., Ruoppolo, M., Pucci, P., Freedman, R. B., and Marino, G. (2000) *Protein Sci. 9*, 525−535.
19. Wedemeyer, W. J., Xu, X., Welker, E., and Scheraga, H. A. (2002) *Biochemistry 41*, 1483−1491.
20. Garel, J.-R. (1978) *J. Mol. Biol. 118*, 331−345.
21. Konishi, Y., and Scheraga, H. A. (1980) *Biochemistry 19*, 1316−1322.
22. Nöppert, A., Gast, K., Muller-Frohne, M., Zirwer, D., and Damaschun, G. (1996) *FEBS Lett. 380*, 179−182.
23. Zhou, J.-M., Fan, Y.-X., Kihara, H., Kimura, K., and Amemiya, Y. (1998) *FEBS Lett. 430*, 275-277.
24. Denisov, V. P., Jonsson, B.-H., and Halle, B. (1999) *Nat. Struct. Biol. 6*, 253−260.
25. Laity, J. H., Shimotakahara, S., and Scheraga, H. A. (1993) *Proc. Natl. Acad. Sci. U.S.A. 90*, 615−619.
26. Creighton, T. E. (1984) *Methods Enzymol. 107*, 305−329.
27. Bruice, T. W., and Kenyon, G. L. (1982) *J. Protein Chem. 1*, 47−58.
28. Thannhauser, T. W., McWherter, C. A., and Scheraga, H. A. (1985) *Anal. Biochem. 149*, 322−330.
29. Rothwarf, D. M., and Scheraga, H. A. (1993) *Biochemistry 32*, 2671−2679.
30. Rothwarf, D. M., and Scheraga, H. A. (1993) *Biochemistry 32*, 2680−2689.
31. Shin, H.-C., and Scheraga, H. A. (2000) *J. Mol. Biol. 300*, 995−1003.
32. Low, L. K., Shin, H.-C., and Scheraga, H. A. (2002) *J. Protein Chem. 21*, 19−27.
33. Lin, S. H., Konishi, Y., Denton, M. E., and Scheraga, H. A. (1984) *Biochemistry 23*, 5504−5512.
34. Altmann, K. H., and Scheraga, H. A. (1990) *J. Am. Chem. Soc. 112*, 4926−4931.
35. Talluri, S., Falcomer, C. M., and Scheraga, H. A. (1993) *J. Am. Chem. Soc. 115*, 3041−3047.
36. Wlodawer, A., Svensson, L. A., Sjolin, L., and Gilliland, G. L. (1988) *Biochemistry 27*, 2705−2717.
37. Carty, R. P., Pincus, M. R., and Scheraga, H. A. (2002) *Biochemistry 41*, 14815−14819.
38. Narayan, M., Welker, E., Wedemeyer, W. J., and Scheraga, H. A. (2000) *Acc. Chem. Res. 33*, 805−812.
39. Houry, W. A., Rothwarf, D. M., and Scheraga, H. A. (1995) *Nat. Struct. Biol. 2*, 495−503.
40. Wedemeyer, W. J., Welker, E., and Scheraga, H. A. (2002) *Biochemistry 41*, 14637−14644.
41. Iwaoka, M., and Scheraga, H. A. (1998) *J. Am. Chem. Soc. 120*, 5806−5807.

BI030152H